Correlation Levels for Measured Indoor 21.5 GHz Channels With a User-Held Handset

Nielsen, Jesper Ødum; Pedersen, Gert Frølund

Published in:
2022 16th European Conference on Antennas and Propagation (EuCAP)

DOI (link to publication from Publisher):
10.23919/EuCAP53622.2022.9768935

Publication date:
2022

Document Version
Accepted author manuscript, peer reviewed version

Correlation Levels for Measured Indoor 21.5 GHz Channels With a User-Held Handset

Jesper Ødum Nielsen, Gert Frølund Pedersen

APMS, Dept. of Electronic Systems, Technical Faculty of IT and Design, Aalborg University, Denmark.
Email: {jni, gfp}@es.aau.dk

***Abstract*—Adaptive beamforming (BF) is essential when mm-wave bands are utilized for mobile communications, where it is important that the channel experienced when BF is applied is as similar as possible to the estimated channel. This work investigates the similarity of the channel at different time-instants using estimates of auto-correlation functions for the instantaneous channel coefficients, based on 21.5 GHz measurements with a smartphone-like mock-up in different indoor corridor scenarios, with and without a user holding the mock-up. The correlation is found to be relatively independent of the location and orientation, with a reduced correlation with a person present. Further, BF is studied based on the 7-element handheld array with a 8.8–24.6 dB gain found for the 1st amplitude percentile obtained with ideal channel state information (CSI). Non-ideal CSI typically reduces both the correlation and the BF gain.**

***Index Terms*—indoor radio propagation, mm-wave channels, adaptive arrays, beamforming, auto-correlation, channel state information**

I. Introduction

The use of cm-wave and mm-wave bands [1] is a new possibility for the fifth generation (5G) of mobile communication networks that are currently being deployed. Frequencies below 30 GHz are attractive due to available spectrum and expected reasonable propagation conditions [2]. However, due to the higher frequencies compared to legacy sub-6 GHz cellular bands, the use of high-gain antennas is necessary [3].

For mobile communications the handheld use-case is important, in which the device and its antennas are close to the user's hand and body, with possible absorption in the human tissue. In addition, the user may also act as scatterer for signals received or transmitted from the device antennas [4].

Due to the changing radio channel, adaptive beamforming (BF) is needed to implement high-gain antennas, where estimation of the channel state information (CSI) is crucial for good performance. Hence, knowledge of correlation properties of the randomly changing channel could be useful during system design. The current work uses channel impulse response (CIR) measurements of an indoor channel at 21.5 GHz from an access point (AP) to an antenna array in a smartphone-like mock-up, which allows to include the effects of a person holding the mock-up and the dynamic effects due to user movements. Based on the measurements, the main contributions of this work are that auto-correlation properties are determined and dependencies on user orientation and location in the environment are analyzed. In addition, BF gain is analyzed using both ideal and delayed CSI, and prediction of the gain based on the correlation level is investigated.

II. Measurements

The measurements used in this work are described in detail in [5], with only a brief description given here of the parts relevant for the current work. All measurements were carried out using the wide-band correlation channel sounding system system described in [6], that was configured to operate in a 100 MHz band centered at 21.5 GHz. This band was chosen based on the 5G candidate bands at the time, and is close to the 24–27 GHz band that was allocated subsequently. The system is setup in a corridor environment with a dual-polarized horn antenna pointing along the corridor, mounted at 2.05 m height near a side wall to mimic an AP.

The corridor has doors to offices along both sides; the side walls are made of plasterboard on metallic frame, and the floor and ceiling are of concrete, with an additional extra light ceiling made of plasterboard on a metallic frame, hiding various pipes, ventilation ducts, *etc.*

The mobile station (MS) is a mock-up handset equipped with $R = 7$ elements, arranged as a uniform linear array (ULA) along the short side of a 110 mm $\times$ 55 mm printed circuit board (PCB). The element separation is around half the wavelength at 21.5 GHz, and the element patterns have a 5 dBi gain roughly towards the user when held as described below. Details of the array design are given in [7].

In the sounding setup, the MS is the receiver (Rx) and the dual-polarized horn is connected to the transmitter (Tx). Tx1 and Tx2 corresponds to the vertical and horizontal polarization, respectively, which are sounded simultaneously. Although the sounder supports multiple parallel Rx branches it is not desirable to have multiple coax cables connected to the mock-up handset, since this will make it difficult to carry and handle naturally during the measurements. Instead a single coax is connected to a 1:8 switch located in the mock-up handset (only 7 elements are connected). The set of CIRs for all 2×7 branch combinations is denoted a channel *snapshot* below. The measurement of one snapshot took 573 μs, and the snapshot rate was 200 Hz, above the Nyquist rate for the expected changes in the channel. In the following a series of $S = 50$ snapshots will be referred to as a *measurement*.

In the setup the Tx is located about halfway in the corridor with the horn pointing towards an about 18 m long section

Presented at the *2022 16th European Conference on Antennas and Propagation (EuCAP).*
DOI: 10.23919/EuCAP53622.2022.9768935

of the corridor, ending in a closed door. Along the corridor section, 10 measurement locations are defined, L1, L2,..., L10, with L1 furthest from the Tx. About halfway there is a bend in the corridor, so that L1–L6 are in non-line of sight (NLOS) and L7–10 are in line of sight (LOS) of the Tx.

The handset was held by a person in so-called data mode, *i.e.*, holding the handset with both hands in front of the body at an angle of about 60° from vertical and a height of about 1.2 m, as if using a smartphone. In order to capture snapshots in different (small-scale) locations, the handset was moved during the measurement in a circular manner, horizontally and while keeping the orientation. The radius of movement was roughly 5 cm, corresponding to about 3.5 wavelengths.

Four orientations were defined. In orientation O1 and O3, the user faces, respectively, away from and towards the Tx, while for orientation O2 and O4 the user faces either side wall.

In total more than 500 measurements were conducted, where all combinations of L1–L10 and O1–O4 are included. Many repetitions were carried out and up to 5 persons were involved, depending on location. Also so-called *free space* measurements were made, where the handset is mounted on a expanded polystyrene foam (EPS) column instead of held by a user, with the column moving to make the handset move in a similar way as for the user-held case.

The measurements for each combination of location and orientation are divided in to groups of two measurement types. The first group "Person" consists of all measurements with a person. Thus, this group may involve different persons and some repetitions. The second group "free space" consists of all measurements in free space, also including repetitions.

III. Data Analysis

For each combination of Tx branch and Rx branch, the measured CIR can be represented as $h'(s,n) = h(s,n) + w(s,n)$, where s and n denote the discrete snapshot and delay index, respectively, and where $h(s,n)$ is the CIR sample and $w(s,n)$ is the noise component. The delay samples are given by $\tau(n) = n\Delta_\tau$ with $n \in \{0,1,\ldots,N-1\}$, $\Delta_\tau = 2.5$ ns and $N = 500$. The snapshots times are $t(s) = s\Delta_t$ where $s \in \{0,1,\ldots,S-1\}$ with $\Delta_t = 5$ ms and $S = 50$ is the number of snapshots in a measurement.

When processing the data it is essential to consider the noise that inevitable will be present in the measured CIR data. The following describes how the signal to noise ratios (SNRs) of the individual snapshots are estimated and how narrow-band (NB) channels are utilized in the processing, repeated here (text until and including the paragraph below (4)) from [8], where a similar analysis and processing of the data was carried out for a different purpose.

Since the noise component cannot be distinguished from the signal component in the following analysis, it is important to ensure a sufficiently high SNR. In order to ensure a large dynamic range the measurement system uses automatic gain control (AGC), which is compensated for during the post-processing for the CIRs. Despite this, a high SNR cannot be guaranteed in all the measurements, due to the highly dynamic channel and the wish to utilize the maximum possible measurement range. When measuring with a sufficiently large distance or number obstacles between the Tx and Rx, the path loss will be too large leading to a low SNR, but exactly where this happens is unknown in advance. Instead one has to rely on experience and testing of the acquired data.

In this work the approach is to estimate the SNR for each CIR snapshot and only include snapshots that have an SNR above a threshold of 15 dB. The instantaneous SNR for snapshot s is estimated by

$$\eta(s) = 10\log_{10}\left[\frac{P_h(s)}{P_w(s)}\right] \tag{1}$$

where the signal and noise power are estimated, respectively, as

$$\begin{aligned} P_h(s) &= \sum_{n=0}^{M-1} |h(s,n)|^2 - M\tilde{\sigma}_w^2(s) \\ P_w(s) &= M\tilde{\sigma}_w^2(s) \end{aligned} \tag{2}$$

where the signal is assumed to be contained in the first $M = 100$ samples of the CIR, corresponding to 250 ns. This was verified by visual inspection of the data. The estimated instantaneous noise density is

$$\tilde{\sigma}_w^2(s) = \frac{1}{K}\sum_{n=0}^{K-1} |h(s,N-n)|^2 \tag{3}$$

i.e., it is estimated from the last $K = 400$ samples of each CIR. Visual inspection reveals that in this part of the CIR the squared magnitude of the samples may be modeled by fluctuations around a mean value, consistent with the assumption that, due to path loss, any signal components in this delay range are much lower than the system noise.

The SNR estimation described above is done for all combinations of Tx branch index, Rx branch index and snapshot. The subsequent processing only considers data with an SNR above the threshold of 15 dB.

NB channels are considered in this work, and hence a discrete Fourier transform (DFT) is applied to the measured CIRs. The sub-channels are all normalized individually over the snapshots, as

$$H(c,t,r,s) = H'(c,t,r,s)\left[\frac{1}{S}\sum_{s=0}^{S-1} |H'(c,t,r,s)|^2\right]^{-1/2} \tag{4}$$

where $H'(c,t,r,s)$ is the transfer function coefficient before normalization for sub-channel c, Tx index t, Rx index r, and snapshot s. Only a subset of the available sub-channels are included in the analysis, chosen based on the known sounding system frequency response. The response was configured to have a 3 dB bandwidth of about 70 MHz and defines the limits of the selected $C = 86$ sub-channels.

Presented at the *2022 16th European Conference on Antennas and Propagation (EuCAP).*
DOI: 10.23919/EuCAP53622.2022.9768935

For each channel combination the auto-correlation function (ACF) is estimated as

$$A'_q(\tau; c, t, r) = \frac{1}{S} \sum_{s=0}^{S-1} H_q(c, t, r, s) H_q^*(c, t, r, s - \tau) \quad (5)$$

where the subscript q refers to the q-th available measurement for the particular combination of location, orientation, and type, not specified here for brevity. The integer time-lag of the ACF is denoted τ. The ACF for transmitter t for the measurement combination is computed as

$$A(\tau; t) = \frac{1}{QCR} \sum_{r=0}^{R-1} \sum_{c=0}^{C-1} \sum_{q=0}^{Q-1} A'_q(\tau; c, t, r) \quad (6)$$

i.e., as the average over all Rx branches, sub-channels and the Q measurements available for the scenario, which varies, as described above, for each combination of location, orientation and type. Note that the number of samples included in the averaging for the ACF in practice may be lower than apparent from (6), if some of the CIRs, and hence corresponding sub-channels involved in (5) have insufficient SNR. In such cases, the ACF of (5) is considered undefined and omitted from the final calculation in (6).

Consider a NB system where the received signal is described by

$$y(c, t, r, s) = H(c, t, r, s) x(s) + v(s) \quad (7)$$

where $x(s)$ and $v(s)$ are, respectively, the symbol transmitted and noise at snapshot s, and where the remaining symbols are as defined above. A BF system can be described as

$$z(c, t, s) = \sum_{r=0}^{R-1} y(c, t, r, s) \xi(c, t, r, s) \quad (8)$$

Using the weights

$$\xi(c, t, r, s) = \exp\left\{-j \angle \left[H(c, t, r, s - d)\right]\right\} / \sqrt{R} \quad (9)$$

where $\angle(\cdot)$ denotes the phase of the argument, and considering an Rx system leads to an equal-gain combining (EGC) system [9]. The assumed knowledge of the phase of all the Rx branches is referred to as CSI in the following. In the ideal case the integer $d = 0$ and the weighting aligns the phases of the individual Rx branch outputs. If $d > 0$ the CSI is delayed, simulating a case where the CSI is obtained via estimation, *e.g.*, using transmission of pilot symbols. The corresponding delay is $d\Delta_t = d \cdot 5$ ms. This work analyzes statistics of the EGC output based on vectors formed by concatenating values of $|z(c, t, s)|$ for all combinations of sub-channels, snapshots, and any measurement repetitions, where snapshots with insufficient SNR are omitted. Similarly, statistics of $|H(c, t, r, s)|$ are used as a reference, representing a system without combiner.

It is noted that the sub-channels for a measurement may be correlated, depending on the channel properties, and hence the samples are not necessarily of the same value in the analysis.

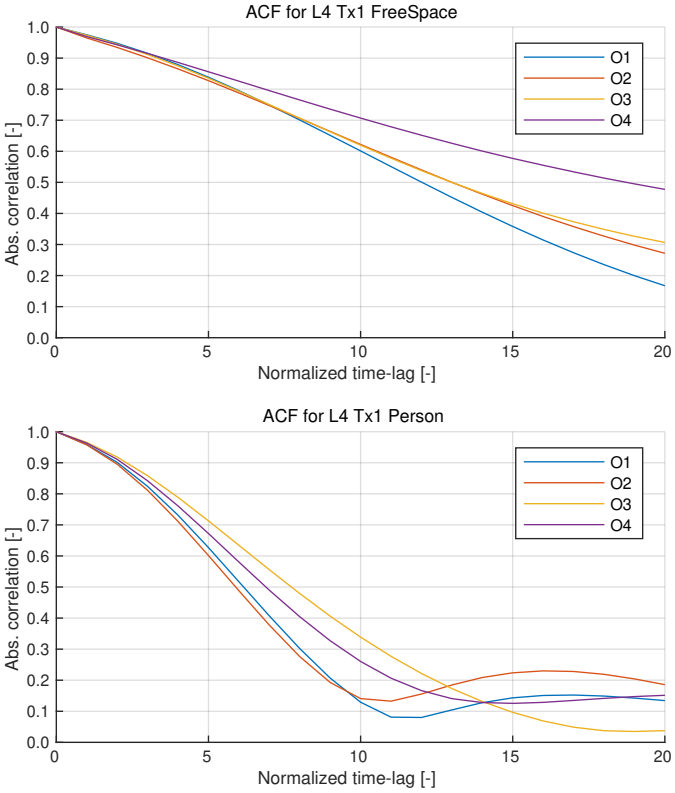

Fig. 1. Estimated ACF curves for different orientation in the scenario L4, Tx1, (top) in free space and (bottom) with person. The time-lag is normalized to the 5 ms sampling interval.

IV. Results

A. Auto-correlation

Fig. 1 shows example ACFs estimated for Tx1 at L4. The correlation levels are generally higher for free space compared to the person case, *e.g.*, with a level about 0.85 at lag 5 for the free space case compared to about 0.6-0.7 for the person case.

An overview of the variation in the ACF is given in Fig. 2 where the correlation is shown for a lag of 5 samples (corresponding to 25 ms), for each combinations of location, orientation, type and Tx. The correlation level is relatively independent of the location, despite being a mix of LOS and NLOS scenarios. For free space the correlation level is generally above 0.8, and the orientation of the device/user in the environment is noticed not to have a strong influence, except at L7 where the level is lower for O2 and O4.

The presence of a person has a de-correlating effect, lowering the average correlation from about 0.83 in free space to about 0.65 with a person. The orientation of the person does not have a strong influence, expect at L2.

It is noted that at some locations, especially L2 and L3, data points are unavailable, since the ACF cannot be estimated due to insufficient SNR, as explained in Section III.

Presented at the *2022 16th European Conference on Antennas and Propagation (EuCAP).*
DOI: 10.23919/EuCAP53622.2022.9768935

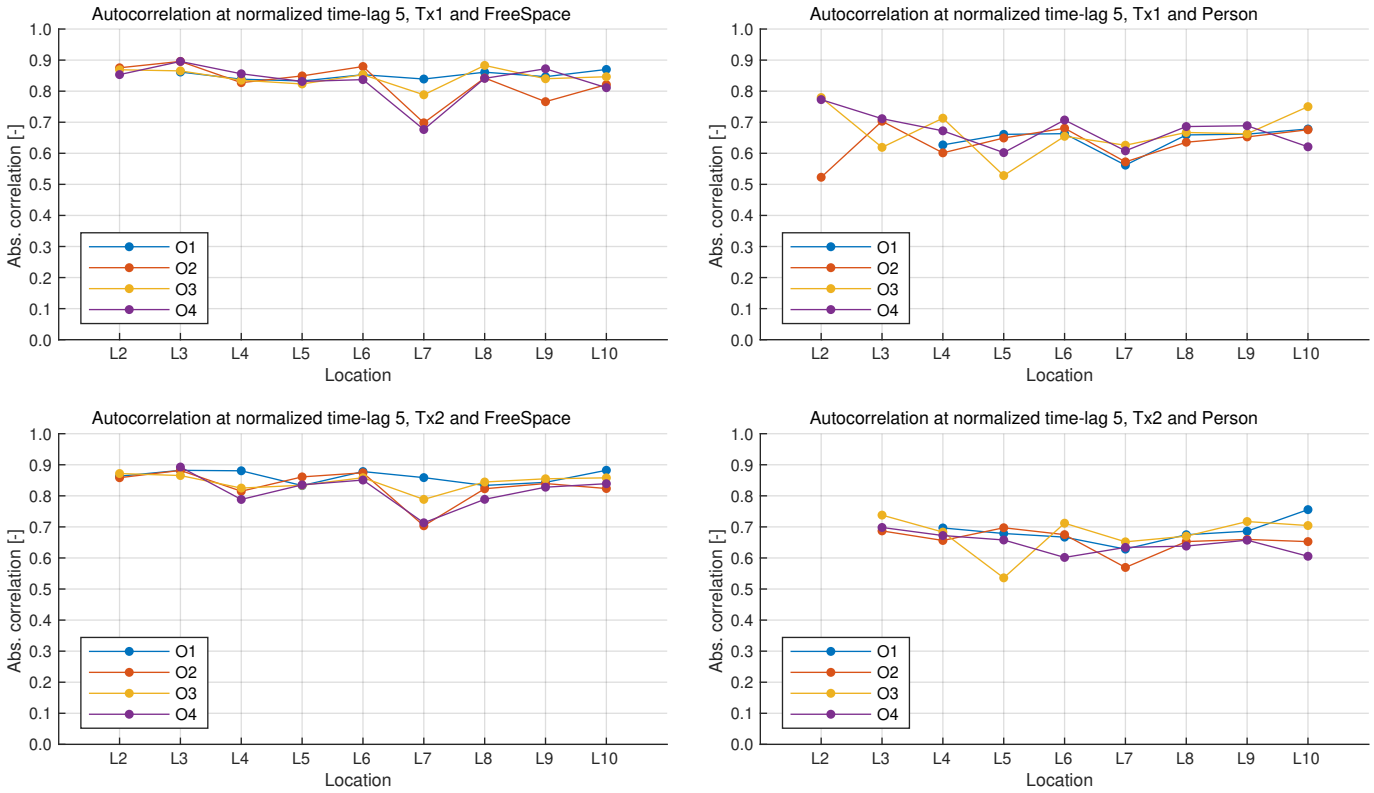

Fig. 2. ACF value at normalized time-lag 5 (25 ms) for all combinations of location, orientation, measurement type and Tx. Note only points represent data, lines are only for visual aid.

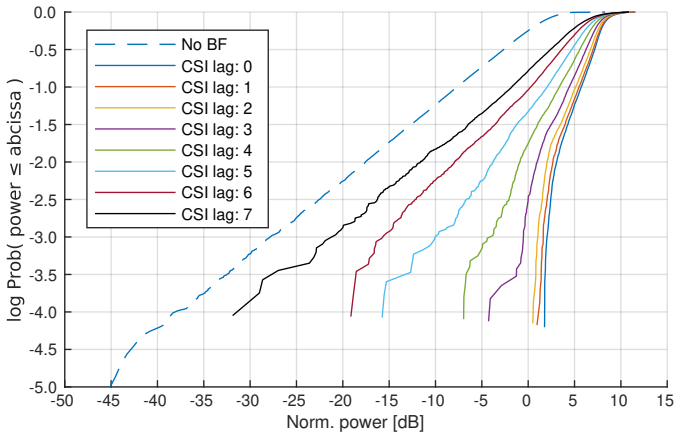

Fig. 3. Estimated CDF curves for the amplitude obtained with BF using CSI assuming different time-delay (norm. to 5 ms), in the scenario L4, O2, Tx2, with person.

B. Beamforming

As illustrated by the ACF in Fig. 1, increasing the time-lag leads to a decreasing correlation between samples of the channel. Hence, it can be expected that increasing the time between setting BF weights and applying them to the channel will lead to, in an average sense, reduced amplitudes. Fig. 3 shows examples of CDF curves estimated from the amplitudes obtained when using BF with the 7-element array, as described in Section III. The dashed line is the amplitude CDF for the case when no BF is applied (estimated using all Rx channels), showing that the channels have a bit less frequent deep fades than a theoretical Rayleigh channel. Using BF with a CSI delay of zero results in a large diversity gain of some 20 dB at a probability level of 10^{-2}, which is reduced to about 6 dB when the CSI lag is 7.

A scatter plot is shown in Fig. 4, where the points show the BF gain versus the correlation level. The BF gain is defined as the difference of the 1st percentile of the absolute amplitude for the BF output and the reference channels, respectively, similarly to comparing the CDF curves at the 10^{-2} level. The points in Fig. 4 represent all the available combinations of location, orientation, Tx, and measurement type, where the different colors indicate the assumed CSI lag. The points in blue for CSI lag 0 represents the performance in ideal conditions, where it is noticed that the BF gain varies from about 8.8 dB to 24.6 dB depending on the scenario. When a CSI lag of 1 is assumed, the correlation decreases to about 0.95-0.98, but the range of BF gain values is almost unchanged from the ideal case. Also for a CSI lag of 2, the gain range is almost the same, but the range of correlation values is widened.

By choosing all CSI delays $0, 1, \ldots, 10$ more data point are obtained for the scatter plot, as shown in Fig. 5. Clearly there is a general tendency of reduced BF gain for lower correlation values, as indicated by the line showing a linear least squares

Presented at the *2022 16th European Conference on Antennas and Propagation (EuCAP).*
DOI: 10.23919/EuCAP53622.2022.9768935

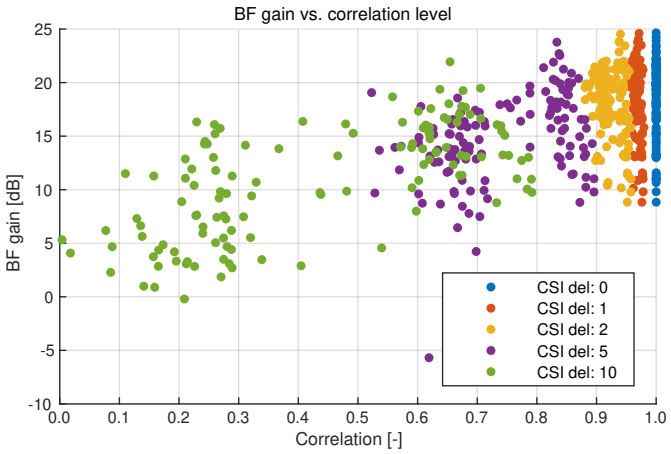

Fig. 4. BF gain at amplitude CDF level 10^{-2} versus ACF level for different assumed CSI time-delay (norm. to 5 ms). Data points are for all combinations of location, orientation, measurement type, and Tx.

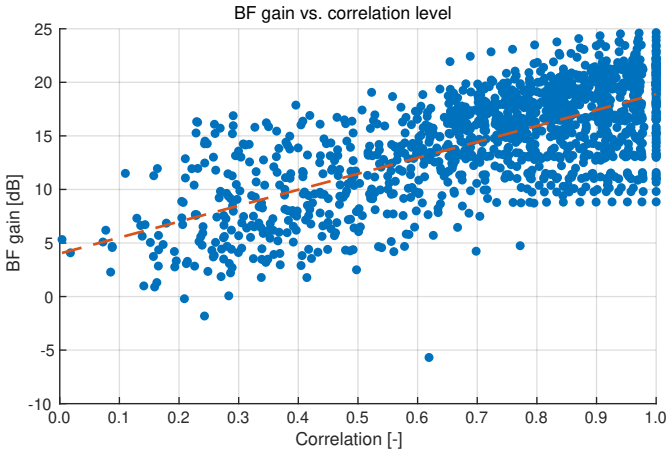

Fig. 5. BF gain at amplitude CDF level 10^{-2} versus ACF level for assumed CSI time-delay (norm. to 5 ms) in the range 0–10. Data points are for all combinations of location, orientation, measurement type, and Tx. A linear regression line is also shown.

fit. However, the linear fit is not very precise in predicting the BF gain from the correlation, due to the large variation in the data points around the line.

V. Conclusions

This work investigates the channel between an access point (AP) and a handheld device operating in the 21.5 GHz band in an indoor corridor environment. The focus is on characterizing the similarity of the channel coefficients experienced at different time-instances, which is important, *e.g.*, for a system estimating the channel for later use in beamforming (BF). The work is based on wide-band measurements in scenarios defined by combinations of 9 locations, 4 orientations, 2 AP polarizations and with or without a user holding the mock-up handset.

The auto-correlation is a way to characterize the similarity of the channel coefficients. Auto-correlation functions were estimated for all the scenarios, where it was found that the correlation (for fixed lag) was relatively independent of the different locations and orientations in the environment. The average correlation was 0.83 in free space and 0.65 with a person present, both for a lag of 25 ms. Thus, the presence of a person generally had a de-correlating effect.

BF was investigated in the form of equal-gain combining, where the instantaneous weights are set from the channel state information (CSI), assumed known with a specified time-lag. BF gains estimated from amplitude 1st percentiles were 8.8–24.6 dB, depending on the scenario and for ideal zero-lag CSI. For non-zero lags the channel auto-correlation generally decreases, with observed values in the 1–0 range for lags 0–50 ms. A linear fit of the BF gain versus the correlation was obtained, with a slope of 14.9 dB/correlation unit. However, the linear fit is not very precise in predicting the BF gain from the correlation.

Acknowledgment

This work was supported by the Danish National Advanced Technology Foundation project “Virtuoso.”

References

[1] Q. C. Li, H. Niu, A. T. Papathanassiou, and G. Wu, “5G network capacity: Key elements and technologies,” *IEEE Vehicular Technology Magazine*, vol. 9, no. 1, pp. 71–78, 2014.

[2] M. Samimi, K. Wang, Y. Azar, G. N. Wong, R. Mayzus, H. Zhao, J. K. Schulz, S. Sun, F. Gutierrez, and T. S. Rappaport, “28 GHz angle of arrival and angle of departure analysis for outdoor cellular communications using steerable beam antennas in new york city,” in *Vehicular Technology Conf. (VTC Spring), 2013 IEEE 77th*, June 2013, pp. 1–6.

[3] W. Roh, J. Seol, J. Park, B. Lee, J. Lee, Y. Kim, J. Cho, K. Cheun, and F. Aryanfar, “Millimeter-wave beamforming as an enabling technology for 5G cellular communications: theoretical feasibility and prototype results,” *IEEE Commun. Mag.*, vol. 52, no. 2, pp. 106–113, 2014.

[4] I. Syrytsin, S. Zhang, G. F. Pedersen, K. Zhao, T. Bolin, and Z. Ying, “Statistical investigation of the user effects on mobile terminal antennas for 5G applications,” *IEEE Trans. Antennas Propag.*, vol. 65, no. 12, pp. 6596–6605, 2017.

[5] J. Hejselbæk, J. Ø. Nielsen, W. Fan, and G. F. Pedersen, “Measured 21.5 GHz indoor channels with user-held handset antenna array,” *IEEE Trans. Antennas Propag.*, vol. 65, no. 12, pp. 6574–6583, Dec 2017.

[6] J. Ø. Nielsen, W. Fan, P. C. F. Eggers, and G. F. Pedersen, “A channel sounder for massive MIMO and MmWave channels,” *IEEE Commun. Mag.*, vol. 56, no. 12, pp. 67–73, December 2018.

[7] N. Ojaroudiparchin, M. Shen, S. Zhang, and G. Pedersen, “A switchable 3d-coverage phased array antenna package for 5g mobile terminals,” *IEEE Antennas Wireless Propag. Lett.*, vol. 15, pp. 1747 – 1750, Feb. 2016.

[8] J. Ødum Nielsen and G. Frølund Pedersen, “Amplitude distributions of measured 21.5 GHz indoor channels for a handheld array,” in *2021 15th European Conf. Antennas and Propagation (EuCAP)*, 2021, pp. 1–5.

[9] R. Vaughan and J. B. Andersen, *Channels, propagation and antennas for mobile communications*. London, United Kingdom: The Institution of Electrical Engineers, 2003.

Presented at the *2022 16th European Conference on Antennas and Propagation (EuCAP).*
DOI: 10.23919/EuCAP53622.2022.9768935